2009 American Control Conference
Hyatt Regency Riverfront, St. Louis, MO, USA
June 10-12, 2009

Extremum Seeking With Very Slow or Drifting Sensors

Nima Ghods and Miroslav Krstic

Abstract— **Slow sensors arise in many applications, including sensing of concentrations of chemicals in tracking of contaminant plumes. Slow sensors are often the cause of poor performance and a potential cause of instability. In this paper we design a modified extremum seeking scheme to account for and even to exploit slow sensor dynamics. We also consider the worst case, which is sensor dynamics governed by a pure integrator. We provide stability results for several distinct variations on our ES scheme. We use metal-oxide microhotplate gas sensors as a real world example of slow sensor dynamics, model the sensor based on experimental data, and provide extremum seeking simulation results employing the identified sensor model.**

I. Introduction

Recent advances in extremum seeking have shown it to be a powerful tool in real time non-model based control and optimization [3], [17], [19], [20], [21]. Success has been achieved in compensating slow actuator dyncamics [22], [23], [6], [4], [5], but no work has been done with extremum seeking for plants with slow sensor dynamics, or, in the extreme case, sensors governed by a pure integrator (drifting sensors). In this paper we introduce a new idea of how to extend the applicability of extremum seeking to plants with a slow or drifting sensor.

For simplicity, we consider a single-parameter extremum seeking problem with a static map, but with sensor dynamics. The classical extremum seeking scheme [1] is modified by observing that the integrator, a key adaptation element, is already present in sensor dynamics, if they are governed by a pure integrator. We perform an appropriate (time-varying) swap of the integrator block and the demodulation block (Section III), and as a result obtain a scheme where the map output converges to the extremum fast, while the sensor output may converge slowly, or it may even drift to infinity.

Stability and simulation results are presented first for a system with a slow sensor (Section IV). This is followed by results for a sensor governed by a pure integrator (Section V). (These results do not imply one another.)

Traditional methods for gas plume seeking using slow metal oxide sensors [11], [12], [13] (reviewed in Section II) either wait for a big enough change in the sensor reading or for the sensor reading to settle before they act. Most of these search methods ([2], [14], [15]) are based on mimicking insect behavior (mainly moths) to localize source of odor without much consideration of the sensor dynamics. The modified ES scheme reacts to the sensor reading continuously, which allows the overall system to converge to an optimum much faster than the sensor settling time.

Our compensation of slow sensor dynamics does *not* amount to employing a differentiator after the sensor to cancel the integrator in the sensor and act on the trend of the signal, rather than on the value of the signal. This approach would result in amplification of noise. Instead, our approach *leverages* the integrator action in the sensor, to have it assume the role of the tuning element in the extremum seeking loop. We highlight this by considering both a version of the modified scheme with the standard washout filter in the loop and a version without the washout filter, proving stability in each case.

To show the capabilities of the modified extremum seeking scheme with the metal oxide sensors we consider the realistic one dimensional problem of trying to localize a gas leak along a pipe with a single moving sensor.

II. Model of a Metal Oxide Sensor

Due to their small size, metal oxide based microhotplate sensors can be used to develop a portable, sensitive, and low-cost gas monitoring system to detect, for example, leakage of hazardous gases. Modeling metal oxide microhotplate sensor dynamics accurately can prove to be very difficult, as seen in [8], [9], and [10]. In this section we make some reasonable assumption to simplify the complicated models. The basic premise of the sensor model in [8], [9], and [10] is that the sensor reading is driven by an exponential of the concentration of several gases, and the gas concentrations are governed by several coupled ordinary differential equations (corresponding to several chemical reactions) if the temperature is constant. The problem that we are concerned with in this paper is locating the maximum of a single gas with little fluctuation in temperature. Tests were performed to better understand the leading dynamics of the sensor. A gas with a certain concentration was released at 30 [sec] into the experiment then the gas was flushed out at 600 [sec]. Fig. 1 shows the reaction of a TGS2602 metal oxide microhotplate sensor [7] to ethanol at four different concentrations. Note in Fig. 1 that the sensor reading takes around 120 [sec] to settle, independently of the gas concentration.

From these test we see that the dominant dynamics of the sensor are governed by a first order system,

$$G_{\text{sensor}}(s) = \frac{b}{s+\varepsilon}, \tag{1}$$

where b and ε are positive constants that depend on the sensor and the type of gases. As evident from Fig. 1, there is also an offset parameter in the sensor reading, which does nothing more than shift the plot up or down. After performing several tests we observed that, although ε is positive, its magnitude is quite small (on the order of 10^{-2}), which is apparent in Fig. 1

The authors are with the Department of Mechanical and Aerospace Engineering, University of California, San Diego (krstic@ucsd.edu).

The authors gratefully acknowledge the contribution of Alexander Vergara and Kerem Muezzinoglu for their helpful knowledge of the metal oxide sensors, and the funding support by the Los Alamos National Laboratory and Office of Naval Research (ONR).

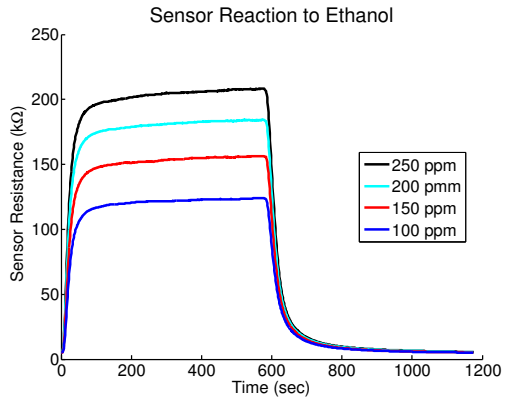

Fig. 1. An example of metal oxide sensor TGS2602 responding to four different concentrations of ethanol.

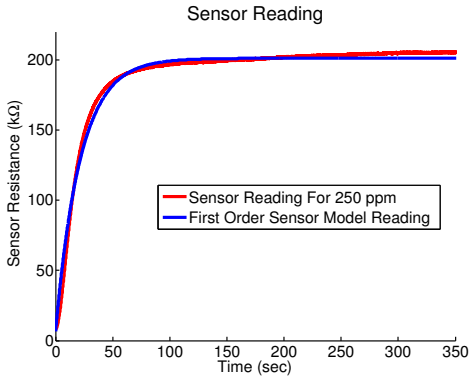

Fig. 2. Comparison of the first order sensor model and the real sensor reaction to ethanol.

where it takes the sensor two minutes to settle. By inspection we set $b = 0.037, \varepsilon = 0.046$ and the offset to 1.6 [kΩ] to get the model for the TGS2602 gas sensor reacting to ethanol. Fig. 2 compares the identified sensor model against the real TGS2602 gas sensor reading. The sensor model parameters change for different gases and different sensors but always stay positive.

III. Extremum Seeking Design for Slow Sensors

We consider applications in which the object is to maximize the output of an unknown nonlinear map $f(\theta)$, by varying the input θ, but where the signal $f(\theta(t))$ is measured through a slow sensor, namely, where only the signal $y(t)$, governed by the ODE

$$\dot{y} = -\varepsilon y + b f(\theta)\,, \tag{2}$$

is measured. Let the maximizing value of θ be denoted as θ^*. This value is unknown and so is $f(\theta^*)$. For simplicity of

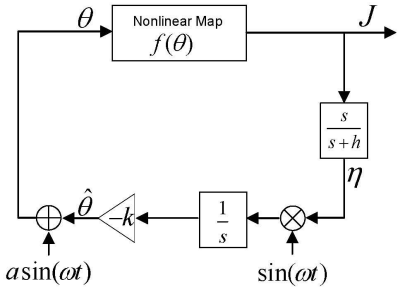

(a) Classical extremum seeking algorithm

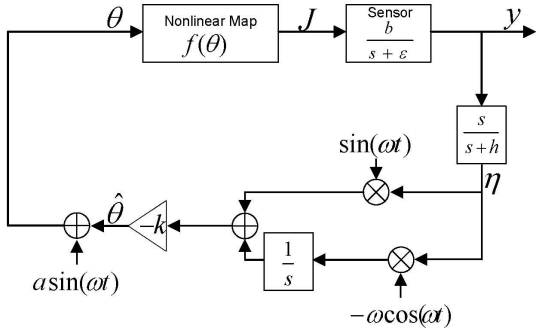

(b) Modified ES for slow sensor

Fig. 3. The modified extremum seeking algorithm (b) applies both to the case with a slow sensor ($\varepsilon > 0$) and to the case with a sensor modeled as a pure integrator, which we also refer to as a 'drifting sensor' ($\varepsilon = 0$). In both cases, the washout filter is optional (both $h > 0$ and $h = 0$ are permissible).

our analysis we assume that the nonlinear map is quadratic,

$$f(\theta) = f^* - q_\theta(\theta - \theta^*)^2\,, \tag{3}$$

where, besides θ^* and f^* being unknown, q_θ is an unknown positive constant.

We modify the classical extremum seeking scheme, which allows fast sensor dynamics, to work with very slow sensors, and, in the extreme case, with sensors governed by a pure integrator, namely drifting sensors. We start with a key observation that an integrator is already a part of the classical extremum seeking loop in Fig. 3(a). We need to modify the scheme so that the sensor itself is performing the task of this integrator (and then eliminate this integrator). To do this, we need to swap the integrator and the multiplication by $\sin(\omega t)$ in Fig. 3(a), i.e., to move the integrator upstream in the signal path. This is not a simple swap of linear blocks because a *multiplication* by a time varying signal is involved. However, using integration by parts, we get that

$$\int_0^t \eta(\tau)\sin(\omega\tau)d\tau = \sin(\omega t)\int_0^t \eta(\tau)d\tau - \omega\int_0^t \cos(\omega\tau)\int_0^\tau \eta(\sigma)d\sigma d\tau\,. \tag{4}$$

We use this observation to convert the scheme in Fig. 3(a) to the scheme in Fig. 3(b), where the guiding idea is that the sensor is a pure integrator, namely, $\varepsilon = 0$. As we shall see, this modification also works when $\varepsilon > 0$.

In the following sections we will show, using averaging theory, that the modified extremum seeking scheme drives θ to a small neighborhood of θ^*, using just the output of the sensor and without any knowledge of the map parameters or the sensor parameters (except for the knowledge that $q_\theta > 0$ and ε is small or zero).

IV. Slow Sensor

In this section we study the case of a slow sensor ($\varepsilon > 0$ but small). We consider both the ES scheme with a washout filter ($h > 0$) and without a washout filter ($h = 0$). In the next section we address the same two cases but for a sensor modeled as a pure integrator ($\varepsilon = 0$).

Let $\hat{\theta}$ be the estimate of θ^* and $\tilde{\theta}$ be the error,

$$\tilde{\theta} = \hat{\theta} - \theta^* \quad (5)$$

$$\theta = \hat{\theta} + a\sin(\omega t)\,, \quad (6)$$

which yields

$$\theta - \theta^* = \tilde{\theta} + a\sin(\omega t)\,. \quad (7)$$

From Fig. 3 we write the equation for $\hat{\theta}$ in terms of η

$$\hat{\theta} = k\left(\eta\sin(\omega t) + \frac{1}{s}[-\eta\omega\cos(\omega t)]\right)\,, \quad (8)$$

where we mix the time and frequency domain notation by using the brackets $[\cdot]$ to denote that the transfer function acts as an operator on a time-domain function.

To prove stability we are going to look at the three signals $\tilde{\theta}$ (the estimation error), η (the signal after the washout filter), and y (the sensor reading). Assuming the nonlinear map in (3) we write an equation for y in terms of θ, then we apply the washout filter to the sensor output y to get η, and finally we get $\tilde{\theta}$ directly from replacing $\hat{\theta}$ in (5) with (8):

$$y = \frac{b}{s+\varepsilon}\left[f^* - q_\theta(\theta-\theta^*)^2\right] \quad (9)$$

$$\eta = \frac{s}{s+h}[y] \quad (10)$$

$$\tilde{\theta} = k\left(\eta\sin(\omega t) + \frac{1}{s}[-\eta\omega\cos(\omega t)]\right) - \theta^*. \quad (11)$$

Using (7) we can now replace θ with $\tilde{\theta}$ in (9). By rearranging (9) and (10) and multiplying (11) by s we obtain the ODEs

$$\dot{y} = -\varepsilon y + b\left(f^* - q_\theta(\tilde{\theta} + a\sin(\omega t))^2\right) \quad (12)$$

$$\dot{\eta} = -h\eta - \varepsilon y + b\left(f^* - q_\theta(\tilde{\theta} + a\sin(\omega t))^2\right) \quad (13)$$

$$\dot{\tilde{\theta}} = -k\left(h\eta + \varepsilon y - b\left(f^* - q_\theta(\tilde{\theta} + a\sin(\omega t))^2\right)\right)\sin(\omega t)\,. \quad (14)$$

Setting $\tau = \omega t$ we get

$$\frac{dy}{d\tau} = \frac{1}{\omega}\left[-\varepsilon y + bf^* - bq_\theta(\tilde{\theta} + a\sin(\tau))^2\right] \quad (15)$$

$$\frac{d\eta}{d\tau} = \frac{1}{\omega}\left[-h\eta - \varepsilon y + bf^* - bq_\theta(\tilde{\theta} + a\sin(\tau))^2\right] \quad (16)$$

$$\frac{d\tilde{\theta}}{d\tau} = -\frac{1}{\omega}k(h\eta + \varepsilon y - bf^* + bq_\theta(\tilde{\theta} + a\sin(\tau))^2)\sin(\tau)\,. \quad (17)$$

Using the following two identities

$$\frac{1}{2\pi}\int_0^{2\pi}(\tilde{\theta} + a\sin(\tau))^2 d\tau = \tilde{\theta}^2 + \frac{a^2}{2} \quad (18)$$

$$\frac{1}{2\pi}\int_0^{2\pi}(\tilde{\theta} + a\sin(\tau))^2\sin(\tau) d\tau = \tilde{\theta}a, \quad (19)$$

to average (15), (16) and (17) become

$$\frac{dy_{\rm avg}}{d\tau} = \frac{1}{\omega}\left[-\varepsilon y_{\rm avg} + bf^* - bq_\theta\left(\tilde{\theta}^2 + \frac{a^2}{2}\right)\right] \quad (20)$$

$$\frac{d\eta_{\rm avg}}{d\tau} = \frac{1}{\omega}\left[-h\eta_{\rm avg} - \varepsilon y_{\rm avg} + bf^* - bq_\theta\left(\tilde{\theta}^2 + \frac{a^2}{2}\right)\right] \quad (21)$$

$$\frac{d\tilde{\theta}_{\rm avg}}{d\tau} = -\frac{kbaq_\theta}{\omega}\tilde{\theta}_{\rm avg}\,. \quad (22)$$

The equilibrium of the averaged system (20)-(22) is $y^e_{\rm avg} = \frac{b}{\varepsilon}\left(f^* + \frac{q_\theta a^2}{2}\right)$, $\eta^e_{\rm avg} = 0$, and $\tilde{\theta}^e_{\rm avg} = 0$. The Jacobian of (20), (21) at $(y^e_{\rm avg}, \eta^e_{\rm avg}, \tilde{\theta}^e_{\rm avg})$ is

$$J_{\rm avg} = \frac{1}{\omega}\begin{bmatrix} -\varepsilon & 0 & 0 \\ -\varepsilon & -h & 0 \\ 0 & 0 & -kbaq_\theta \end{bmatrix}. \quad (23)$$

Given that the nonlinear map has a maximum ($q_\theta > 0$) and that the sensor is stable ($\varepsilon > 0$) and non-inverting ($b > 0$), it follows that, if we choose $a, \omega, k, h > 0$, the Jacobian (23) is Hurwitz and the equilibrium of the averaged system (20)-(22) is locally exponentially stable. From averaging theorem [16] we get the following result.

Theorem 1: There exists ω^* such that for all finite $\omega > \omega^*$ the system in Fig. 3 with nonlinear map (3) has a unique exponentially stable periodic solution $(y^{2\pi/\omega}(t), \eta^{2\pi/\omega}(t), \tilde{\theta}^{2\pi/\omega}(t))$ of period $2\pi/\omega$ which satisfies

$$\left\|\begin{bmatrix} y^{2\pi/\omega}(t) - \frac{b}{\varepsilon}\left(f^* + \frac{q_\theta a^2}{2}\right) \\ \eta^{2\pi/\omega}(t) \\ \tilde{\theta}^{2\pi/\omega}(t) \end{bmatrix}\right\| \leq O(1/\omega),\ \forall\ t \geq 0. \quad (24)$$

Since $\theta - \theta^* = \tilde{\theta} + a\sin(\omega t) = (\tilde{\theta} - \tilde{\theta}^{2\pi/\omega}) + \tilde{\theta}^{2\pi/\omega} + a\sin(\omega t)$, the theorem implies that the first term is zero, the second term is $O(1/\omega)$, and the third term is $O(a)$. Thus $\limsup_{t\to\infty}|\theta(t) - \theta^*| = O(1/\omega)$. Hence, we get

$$\limsup_{t\to\infty}|f(\theta(t)) - f^*| = O(a^2 + 1/\omega^2)\,, \quad (25)$$

which characterizes the asymptotic performance of the extremum seeking loop in Fig. 3.

Fig. 5 shows a simulations of a moving sensor along the length of a pipe, whose objective is to localize a gas leak on the pipe with the use of sensor-compensated extremum seeking. The extremum seeking parameters were chosen as $\omega = 30$, $a = 0.2$, $k = 10$, and $h = 1$. The plant map, shown in Fig. 4, is modeled in the form $f(\theta) = \frac{\delta^*}{1+p_\theta(\theta-\theta^*)^2}$, with $\delta^* = 250$, $p_\theta = 0.5$, and $\theta^* = 0$ to simulate a more realistic gas distribution of a gas pipe with a leak of 250 ppm of ethanol at position θ^*. We assume the sensor model in (1) with the parameters $\varepsilon = 0.046$ and $b = 0.037$, which were obtained by fitting the model to data from the TGS2620

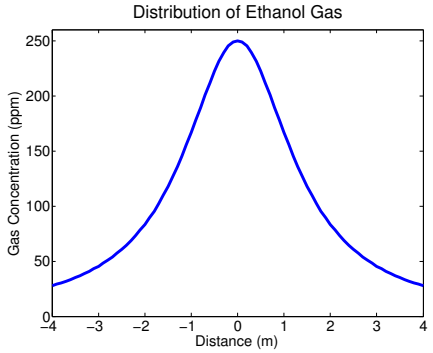

Fig. 4. Gas concentration distribution along the pipe with gas leak at position 0.

gas sensor being exposed to ethanol. The moving sensor starts 3 [m] away form the gas leak. Fig. 5(a) shows the gas concentration at the position of the gas sensor. Fig. 5(b) shows the position of the of the sensor in reference to the gas leak. The nonlinear map output (J) and the sensor position (θ) quickly converge to a periodic motion around f^* and θ^*, respectively. The signal after the washout filter (η), shown in Fig. 5(c), goes to zero.

Note in Fig. 5(d) that the sensor reading converges very slowly. The time interval for which J and $\hat{\theta}$ are shown in Fig. 5 is only one tenth of the time interval on which η and y are shown. This is done in order to display the details of the rapidly convergent sensor position $\hat{\theta}$, while the sensor reading y is about ten times slower. More specifically, even though it takes the sensor reading $120[\text{sec}]$ to settle the extremum seeking algorithm is able to tune $\hat{\theta}$ to achieve maximum output from the nonlinear map in less then $6[\text{sec}]$.

The convergence would be orders of magnitude slower if the algorithm had to wait for the sensor reading to settle every time it wanted to tweak θ.

In some applications the use of washout filters may be undesirable because they act as approximate differentiators and therefore may result in the amplification of noise. We now drop the washout filter and show that the resulting scheme is still stable, namely, the washout filter is used for performance reasons, not for stability reasons, and not to 'cancel' the extremely slow (integrator-like) dynamics of the sensor. The proof for this case (omitted) is very similar to the proof for the case where the sensor is a pure integrator but the ES scheme does employ a washout filter (Theorem 3), with the Jacobian of the averaged system given as

$$J_{\text{avg}} = \frac{1}{\omega}\begin{bmatrix} -\varepsilon & 0 \\ 0 & -kbaq_\theta \end{bmatrix}. \tag{26}$$

Theorem 2: Consider the system in Fig. 3 with the nonlinear map of form (3) and without the washout filter. There exists ω^* such that for all finite $\omega > \omega^*$ the system has a unique exponentially stable periodic solution $(y^{2\pi/\omega}(t), \tilde{\theta}^{2\pi/\omega}(t))$ of period $2\pi/\omega$ which satisfies

$$\left\| \begin{bmatrix} y^{2\pi/\omega}(t) - \frac{b}{\varepsilon}\left(f^* + \frac{q_\theta a^2}{2}\right) \\ \tilde{\theta}^{2\pi/\omega}(t) \end{bmatrix} \right\| \leq O(1/\omega),\ \forall\ t \geq 0\,. \tag{27}$$

Simulation (not included) for the system in Theorem 2 shows convergence rate that is inferior to that of the algorithm with the washout filter (Theorem 1). This convergence rate difference is not captured by the averaging analysis because the approximation accuracy of averaging is low when some of the eigenvalues of the average system are small (due to small ε).

V. Drifting Sensor

Our scheme works even when $\varepsilon = 0$, namely when the sensor is a pure integrator. This is a rather extreme situation of a sensor that responds, but permanently drifts in its value (towards infinity). All that we can achieve in this case is to maximize the sensor's input, since its output never settles.

The stability analysis for this case mimics some parts of the proof for Theorem 1. Assuming the nonlinear map in (3) and setting $\varepsilon = 0$, we write (9) as $y = \frac{b}{s}\left[f^* - q_\theta\left(\tilde{\theta} + a\sin(\omega t)\right)^2\right]$.

Since the sensor output y is not going to settle when its input $\hat{\theta}$ settles, we do not include the sensor output as one of our states for which we are proving convergence. We study only the states $\tilde{\theta}$ and η, whose equations are

$$\frac{d\eta}{d\tau} = \frac{1}{\omega}\left[bf^* - bq_\theta(\tilde{\theta} + a\sin(\tau))^2 - h\eta\right] \tag{28}$$

$$\frac{d\tilde{\theta}}{d\tau} = -\frac{1}{\omega}k(h\eta - bf^* + bq_\theta(\tilde{\theta} + a\sin(\tau))^2)\sin(\tau)\,. \tag{29}$$

Using the identities (18) and (19) we obtain the following averaged equations

$$\frac{d\eta_{\text{avg}}}{d\tau} = \frac{1}{\omega}[bf^* - bq_\theta(\tilde{\theta}^2 + \frac{a^2}{2}) - h\eta_{\text{avg}}] \tag{30}$$

$$\frac{d\tilde{\theta}_{\text{avg}}}{d\tau} = \frac{1}{\omega}[-kbaq_\theta\tilde{\theta}_{\text{avg}}]. \tag{31}$$

The equilibrium of the averaged system (30), (31) is $\eta^e_{\text{avg}} = \frac{b}{h}\left(f^* + \frac{q_\theta a^2}{2}\right)$ and $\tilde{\theta}^e_{\text{avg}} = 0$. The Jacobian of (30), (31) at $(\eta^e_{\text{avg}}, \tilde{\theta}^e_{\text{avg}})$ is

$$J_{\text{avg}} = \frac{1}{\omega}\begin{bmatrix} -h & 0 \\ 0 & -kbaq_\theta \end{bmatrix}. \tag{32}$$

Theorem 3: There exists ω^* such that for all finite $\omega > \omega^*$ the system in Fig. 3 with the nonlinear map of form (3) and $\varepsilon = 0$ in the sensor dynamics has a unique exponentially stable periodic solution $(\eta^{2\pi/\omega}(t), \tilde{\theta}^{2\pi/\omega}(t))$ of period $2\pi/\omega$ which satisfies

$$\left\| \begin{bmatrix} \eta^{2\pi/\omega} - \frac{b}{h}\left(f^* + \frac{q_\theta a^2}{2}\right) \\ \tilde{\theta}^{2\pi/\omega} \end{bmatrix} \right\| \leq O(1/\omega),\ \forall\ t \geq 0\,. \tag{33}$$

Fig. 6 shows a simulation with a sensor $G_{\text{sensor}}(s) = b/s$ with $\theta^* = 0$, $f^* = 1$, $q_\theta = 0.5$, and $b = 1$. The ES parameters are chosen as $\omega = 30$, $a = 0.2$, $k = 10$, and $h = 1$. Fig. 6(a) shows the ability of the sensor-compensated ES scheme to maximize the output of a nonlinear map even with a marginally stable sensor. As shown in Fig. 6(b), $\hat{\theta}$ starts from $\hat{\theta}(0) = 3$ and converges to a periodic motion around $\theta^* = 0$. Fig. 6(c) shows how the signal after the washout filter (η) converges to a periodic motion around

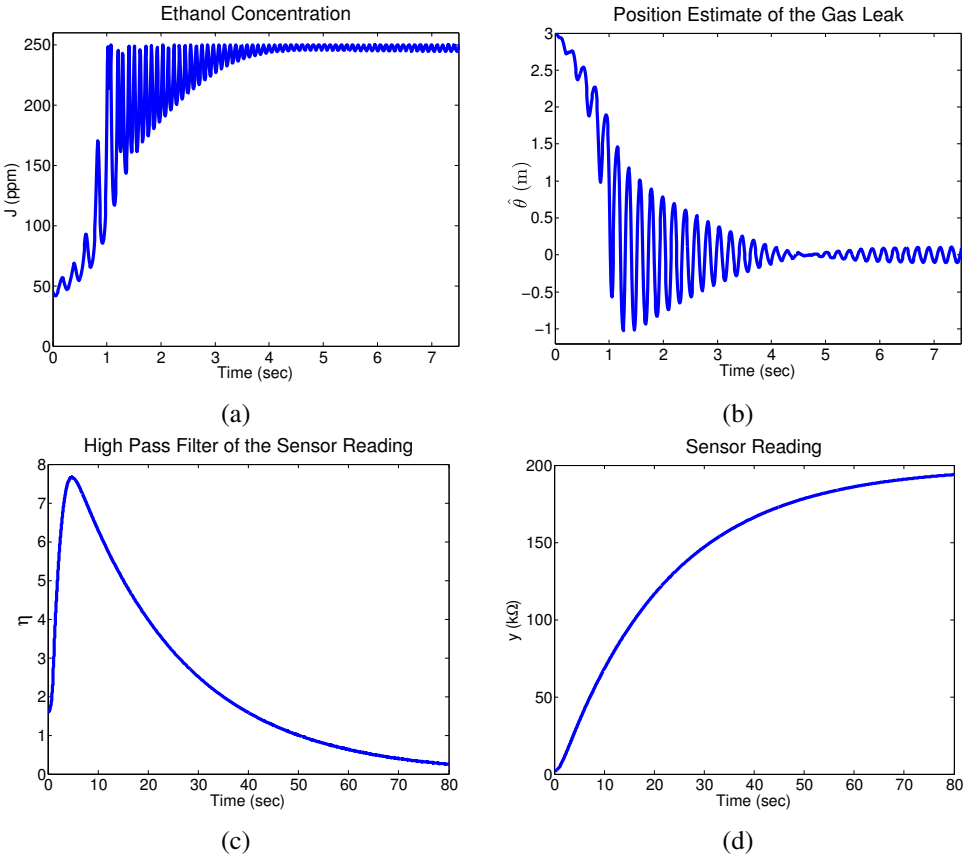

Fig. 5. Simulation results for extremum seeking on a metal oxide sensor model moving along a pipe with a leak showing (a) output of the nonlinear map, (b) the sensor position, and (c) the signal after the high pass filter, and (d) the metal oxide sensor reading. Note that the time interval for which J and $\hat{\theta}$ are shown is only one tenth of the time interval on which η and y are shown. This is done in order to display the details of the rapidly convergent sensor position, while the sensor reading is about ten times slower.

$\eta^e_{\text{avg}} = 1.02$. The response for $y(t)$ is not shown since it drifts in a linear manner towards infinity, as expected.

The scheme studied in Theorem 3 contains a cascade of the sensor's integrator dynamics and of a washout filter. It may appear that the key to the result is that a differentiator cancels an integrator. This is not the case at all, as we illustrate with the next theorem, for the system with $G_{\text{sensor}}(s) = b/s$ and without the washout filter (i.e., with $h = 0$). This simple result is given without a proof, which follows from the fact that the (scalar) Jacobian is $-kbaq_\theta/\omega$ (in the τ time scale).

Theorem 4: Consider the system in Fig. 3 without the washout filter, with ε set to zero in the sensor dynamics, and the nonlinear map of form (3). There exists ω^* such that for all $\omega > \omega^*$ the system has a unique exponentially stable periodic solution $\tilde{\theta}^{2\pi/\omega}(t)$ of period $2\pi/\omega$ which satisfies $\left\|\tilde{\theta}^{2\pi/\omega}(t)\right\| \leq O(1/\omega)$, $\forall\ t \geq 0$.

Simulation results for the system in Theorem 4 are shown in Fig. 7 for $f^* = 1$, $q_\theta = 0.5$, $b = 1$, $\omega = 30$, $a = 0.2$, $k = 10$, and $h = 1$. As expected, θ and f converge to a periodic motion around θ^* and f^*, respectively. The drifting sensor without the washout filter has significant oscillations after settling compared to the case of drifting sensor with the washout filter.

The significance of the result in Theorem 4 are shown in Fig. 7 is that it demonstrates that the modified extremum seeking scheme is not merely acting based on the signal trend/derivative (rather than on the signal value), which would have been the case if the inclusion of a washout filter had turned out to be crucial. Rather than 'canceling' the sensor's integrator, our scheme *leverages* it, by using its presence for the function of tuning of $\hat{\theta}(t)$ in the ES loop.

REFERENCES

[1] K. B. Ariyur and M. Krstic, *Real-Time Optimization by Extremum Seeking Feedback.* Hoboken, NJ: Wiley-Interscience.

[2] J. Belanger and E. Arbas, "Behavioral strategies underlying pheromone-modulated flight in moths: lessons from simulation studies," *Journal of Comparative Physiology* A: *Sensory, Neural, and Behavioral Physiology,* 183(3): 345- 360, 1998.

[3] C. Centioli, F. Iannone, G. Mazza, M. Panella, L. Pangione, S. Podda, A. Tuccillo, V. Vitale, and L. Zaccarian, "Extremum seeking applied to the plasma control system of the Frascati Tokamak Upgrade,"*44th IEEE Conf. on Decision and Ctrl., and the European Ctrl. Conf.,* 2005.

[4] J. Cochran, M. Krstic, "Source seeking with a nonholonomic unicycle without position measurements and with tuning of angular velocity part I: Stability analysis," *IEEE Conf. on Decision and Control*, 2007.

[5] J. Cochran, A.A. Siranosian, N. Ghods and M. Krstic, "Source seeking with nonholonomic unicycle without position measurements and with tuning of angular velocity Part II: Applications," *IEEE Conf. on Decision and Control*, 2007.

[6] J. Cochran, A. Siranosian, N. Ghods, and M. Krstic,"GPS denied source seeking for underactuated autonomous vehicles in 3D," *IEEE International Conf. on Robotics and Automation,* 2008.

[7] Figaro Engineering Inc. Technical information for TGS2620 data sheet, revised 03/05.

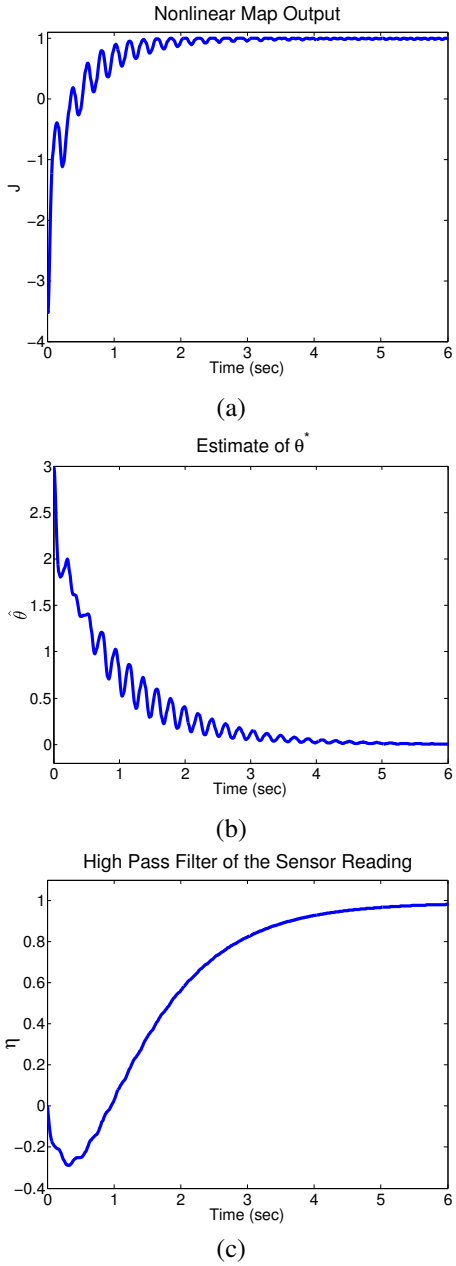

Fig. 6. Simulation results for extremum seeking with $G_{\text{sensor}}(s) = b/s$ showing (a) output of the nonlinear map, (b) the tuned parameter, and (c) the signal after the high pass filter.

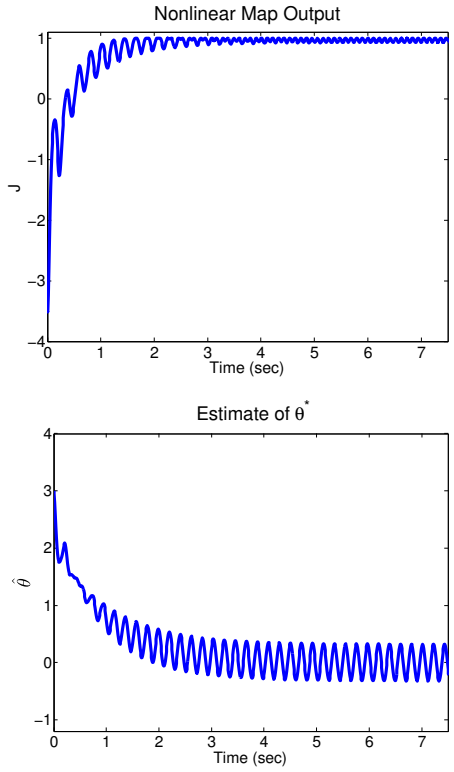

Fig. 7. Simulation results for extremum seeking with $G_{\text{sensor}}(s) = b/s$ without washout filter showing (a) output of the nonlinear map and (b) the tuned parameter.

[8] A. Fort, M. Mugnaini, S. Rocchi, M.B. Serrano-Santos, V. Vignoli, R. "Simplified models for SnO_2 sensors during chemical and thermal transients in mixtures of inert, oxidizing and reducing gases,"*Sens. Actuators B. Chem.,* 2007.

[9] A. Fort, M. Mugnaini, S. Rocchi, M.B. Serrano-Santos, V. Vignoli, R. Spinicci, "Surface state model for conductance responses during thermal-modulation of SnO_2-based thick film sensors. Part I. Model derivation,"*IEEE Trans. Instr. Meas.,* 2006.

[10] A. Fort, M. Mugnaini, S. Rocchi, M.B. Serrano-Santos, V. Vignoli, R. Spinicci, "Surface state model for conductance responses during thermal-modulation of SnO_2-based thick film sensors. Part II. Experimental verification," *IEEE Trans. Instr. Meas.,*2006.

[11] H. Ishida, T. Nakamoto, T. Moriizumi, T. Kikas, and J. Janata,"Plumetracking robots: A new application of chemical sensors," *Biol. Bull.,* vol. 200, pp.222-226, 2001.

[12] H. Ishida, G. Nakayama, T. Nakamoto, T. Moriizumi, "Odor-source Localization In Clean Room By Autonomous Mobile Sensing System," *Sensors and Actuators B:Chemical, Eurosensors IX,* vol.33, pp.115–121, July 1996.

[13] H. Ishida, G. Nakayama, T. Nakamoto, T. Moriizumi, "Controlling a gas/odor plume-tracking robot based on transient responses of gas sensors," *Sens., Proceedings of IEEE,* vol.2, no., pp.1665–1670, 2002.

[14] R. Kanzaki, "Coordination of wing motion and walking suggests common control of zigzag motor program in a male silkworm moth," *Journal of Comparative Physiology* A: *Sensory, Neural, and Behavioral Physiology,* 182(3): 267-276, 1998.

[15] R. Kanzaki, N. Sugi, and T. Shibuya, "Self-generated zigzag turning of Bombyx mori males during pheromonemediated upwind walking" *Zoological Science,* 9(3): 515-527, 1992.

[16] H. Khalil, *Nonlinear Systems,* Prentice-Hall, 2002.

[17] R. King, R. Becker, G. Feuerbach, L. Henning, R. Petz, W. Nitsche, O. Lemke, and W. Neise, "Adaptive flow control using slope seeking," *14th IEEE Mediterranean Conf. on Ctrl.Automation,* 2006.

[18] Y. Li, A. Rotea, G. T.-C. Chiu, L. Mongeau, and I.-S. Paek, "Extremum seeking control of a tunable thermoacoustic cooler," *IEEE Trans. Contr. Syst. Technol.,* vol. 13, pp. 527-536, 2005.

[19] Y. Ou, C. Xu, E. Schuster, T. Luce, J. R. Ferron, and M. Walker, "Extremum-seeking finite-time optimal control of plasma current profile at the diii-d tokamak," *2007 American Ctrl. Conf.,* 2007.

[20] Y. Tan, D. Nesic, and I. M. Y. Mareels, "On non-local stability properties of extremum seeking controllers," *Automatica,* vol. 42, pp. 889-903, 2006.

[21] M. Tanelli, A. Astolfi, and S. Savaresi, "Non-local extremum seeking control for active braking control systems," *Conf. on Con. App.,* 2006.

[22] C. Zhang, A.A. Siranosian, and M. Krstic, "Extremum seeking for moderately unstable systems and for autonomous vehicle target tracking without position measurements," *Automatica,* vol. 43, pp. 1832–1839, 2007.

[23] C. Zhang, D. Arnold, N. Ghods, A.A. Siranosian and M. Krstic, "Source seeking with nonholonomic unicycle without position measurement - Part I: Tuning of forward velocity," *IEEE Conf. on Decision and Control,* 2006.